

Performance-Based Seismic Design of Controlled Rocking Steel Braced Frames. II: Design of Capacity-Protected Elements

Lydell Wiebe¹ and Constantin Christopoulos, M.ASCE²

Abstract: Controlled rocking steel braced frames (CRSBFs) are intended to have a self-centering response that avoids damage to main structural elements. To ensure that all nonlinearity is confined to the intended elements at the rocking joint, the frame must be adequately capacity designed. This requires accurate predictions of the peak forces that are likely to develop in all members of the frame while the rocking mechanism reaches its peak rotation. Previous studies have shown that the peak forces in CRSBF members are likely to be strongly influenced by higher mode effects, but these effects can be mitigated by designing multiple nonlinear mechanisms. This paper proposes methods for estimating the peak forces in frame elements, designing an additional mechanism if it is desired to mitigate higher mode effects, and predicting the reduction in response that will be achieved by adding this mechanism. The methods are validated by designing buildings with two, six, and 12 stories, including three alternative designs that use multiple mechanisms to mitigate the higher mode effects. The six frames are modeled using OpenSees and are subjected to 44 ground motions at the maximum considered earthquake level. The peak forces in the taller frames without additional mechanisms are dominated by higher mode effects, but these effects can be estimated using the proposed method. These forces can also be reduced by designing multiple mechanisms, and the proposed method provides a reasonable design-level prediction of this force reduction. DOI: [10.1061/\(ASCE\)ST.1943-541X.0001201](https://doi.org/10.1061/(ASCE)ST.1943-541X.0001201). © 2014 American Society of Civil Engineers.

Author keywords: Performance-based seismic design; Self-centering systems; Controlled rocking steel braced frames; Higher mode effects; Multiple force-limiting mechanisms; Capacity design; Seismic effects.

Introduction

Many lateral force-resisting systems for buildings can be designed economically to provide life safety during a design-level earthquake, but most of these systems are expected to be difficult to repair after a moderate or larger event. Therefore, alternative self-centering systems are being developed to avoid damage and residual deformations. One such system is a controlled rocking steel braced frame (CRSBF), which has been studied experimentally (Midorikawa et al. 2006; Tremblay et al. 2008a; Ma et al. 2010; Sause et al. 2010; Wiebe et al. 2013a, b; Eatherton et al. 2014) and has also been implemented in practice (Gledhill et al. 2008; Mar 2010; Latham et al. 2013; Tait et al. 2013). Part I (Wiebe and Christopoulos 2014) proposes a general framework for the design of CRSBFs and validates a method for designing the base rocking joint to achieve a predetermined maximum response, assuming that all members of the CRSBF were adequately designed to remain linear elastic.

Although CRSBFs can withstand multiple large earthquakes without structural damage, studies have also shown that the seismic force demands on CRSBFs may not be effectively limited by the rocking mechanism because of higher mode effects. Methods for estimating the peak seismic forces in CRSBFs, including

the influence of the higher modes, have been proposed by Roke et al. (2009), Eatherton and Hajar (2010), and Ma et al. (2011). Higher mode effects can be mitigated by designing multiple force-limiting mechanisms, as was demonstrated in a large-scale shake table test program (Wiebe et al. 2013a, b). However, no proposals have previously been made for the design of multiple force-limiting mechanisms to mitigate higher mode effects in CRSBFs.

This paper begins by developing a theory-based method for estimating the peak seismic forces, including higher mode effects, in the members of a CRSBF. The method is intended to be applied at the preliminary design stage: it does not require any structural modeling and can easily be implemented in a spreadsheet. If this method shows that higher mode effects dominate the response, a designer may wish to design one or more additional force-limiting mechanisms.

This paper also presents a method for designing an upper rocking joint or a nonlinear brace to control the peak forces in the system. The paper validates these proposals by applying them to example designs of buildings with two, six, and 12 stories. The buildings are modeled using *OpenSees*, and the peak system forces at the maximum considered earthquake (MCE) level are compared to the design estimates. The influence of an additional force-limiting mechanism on the peak displacement response is also discussed.

Method to Estimate Peak Element Forces

Although code-based lateral force distributions can be used to relate the design base shear to the design base overturning moment, these distributions do not capture the shapes of the nonlinear dynamic story shear and overturning moment envelopes, which are often strongly influenced by the higher modes

¹Assistant Professor, Dept. of Civil Engineering, McMaster Univ., 1280 Main St. W, Hamilton, ON, Canada L8S 4L7 (corresponding author). E-mail: wiebel@mcmaster.ca

²Professor, Dept. of Civil Engineering, Univ. of Toronto, ON, Canada M5S 1A4.

Note. This manuscript was submitted on April 16, 2014; approved on October 3, 2014; published online on November 17, 2014. Discussion period open until April 17, 2015; separate discussions must be submitted for individual papers. This paper is part of the *Journal of Structural Engineering*, © ASCE, ISSN 0733-9445/04014227(11)/\$25.00.

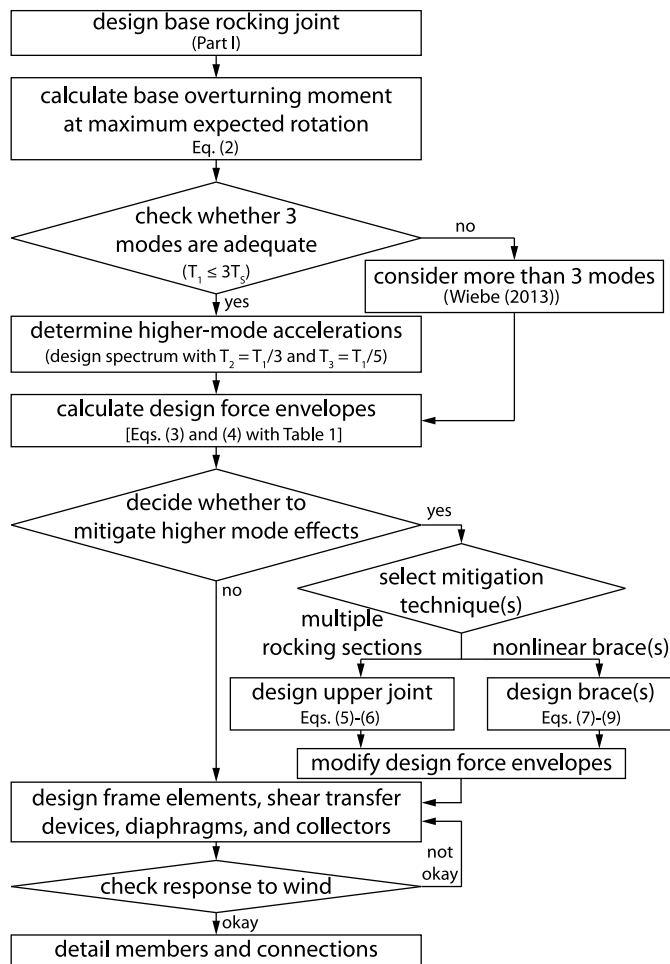


Fig. 1. Proposed capacity design process

(e.g., Wiebe et al. 2013a, b). As an alternative, this paper proposes a procedure that is based on an analogy to continuum shear beams with uniformly distributed mass and elasticity, as detailed by Wiebe (2013). The steps of the proposed capacity design method are shown in Fig. 1 and discussed in the following subsections.

Although this paper considers only lateral modes when referring to higher mode effects, the impact and uplift associated with rocking can also excite vertical modes of vibration. Pollino and Bruneau (2008) have proposed equations to estimate these effects without nonlinear time-history analysis for bridge piers where the mass is concentrated in one location. However, if the CRSBF is designed to avoid carrying significant gravity load, as is recommended (Wiebe and Christopoulos 2014), the dynamic effects of impact are unlikely to substantially increase the peak member force demands (Wiebe 2013). To define the maximum allowable gravity load on the CRSBF before impact effects need to be considered, the following limit is defined based on comparing the maximum compression in the first-story column without any dynamic amplification to the compression in that column at zero base rotation if a dynamic amplification factor of two applies to the gravity load:

$$W_{\text{self}} \leq PT_y - PT_0 \quad (1)$$

where PT_y and PT_0 = yield and initial forces in the posttensioning, respectively, and W_{self} = total vertical load carried by the CRSBF. Similarly, it is proposed that vertical ground

accelerations can be neglected for the design of the CRSBF if Eq. (1) is satisfied.

Calculation of Base Overturning Moment at Maximum Expected Rotation

The base overturning moment associated with θ_{max} , the maximum expected base rotation at the MCE level, is calculated as

$$M_{b,\text{max}} = W_{\text{self}}d_W + \sum(ED_\theta \times d_{ED}) + \sum(PT_\theta \times d_{PT}) \quad (2)$$

where ED_θ and PT_θ = forces in the energy dissipation and posttensioning elements at θ_{max} , including the effects of cyclic strain hardening; and where d_W , d_{ED} , and d_{PT} = minimum distances from the rocking toe to the line of action of the self-weight, each energy dissipation element, and each posttensioning element, respectively.

Checking whether Three Modes are Adequate for Design Envelopes

Wiebe (2013) showed that the response of a structure that behaves like a shear beam (typical low-rise to midrise buildings) may be computed using only the first three modes if $T_1 \leq 3T_S$, where T_1 , the fundamental period, may be estimated as $0.07h_n^{0.75}$ (Kwon and Kim 2010), and where T_S is the corner period of the acceleration spectrum, calculated according to ASCE 7-10 (ASCE 2010). If $T_1 > 3T_S$, modes beyond the third should be included by referring to the equations given by Wiebe (2013). The number of modes is considered to be limited to the number of floor levels.

Determination of Higher-Mode Spectral Accelerations

The spectral accelerations associated with each mode are then determined. Wiebe (2013) showed that the higher-mode periods of a shear beam are nearly independent of the base rotational restraint. Thus, the second-mode and third-mode periods can be estimated as $T_2 = T_1/3$ and $T_3 = T_1/5$, respectively. Although these period estimates could be updated based on the results of modal analysis after the frame has been designed, the examples in this paper suggest that reasonable design estimates of the peak forces are found using these simplifications.

Calculation of Story Shear and Overturning Moment Design Envelopes

Based on the above calculations, the modal contributions to the shear force and overturning moment envelopes (V_{max} and M_{max} , respectively) are found using the equations given in Table 1, which are based on the theoretical modal properties of a cantilevered shear beam with uniformly distributed mass and stiffness and are fully developed by Wiebe (2013). These equations do not require a structural model of the CRSBF because they use only the overstrength base overturning moment resistance ($M_{b,\text{max}}$), the height of each story above the base (z), the height of the CRSBF (H), the tributary seismic mass (W_{trib}/g), and the five-percent-damped spectral accelerations at one-third and one-fifth of the fundamental period [$S_a(T_1/3)$ and $S_a(T_1/5)$]. It is recommended to account for uncertainties in the ground motion by targeting the 84th-percentile acceleration spectrum rather than the median acceleration spectrum. For the suite of FEMA P695 records (FEMA 2009), this results in a spectral amplification of approximately 1.5 at periods of less than 2 s.

Table 1. Modal Contributions to Design Envelopes

Parameter	Mode	Equation
Story shear	First mode	$V_{1,\max}(z) = \frac{3}{2} \left(\frac{M_{b,\max}}{H} \right) \left[1 - \left(\frac{z}{H} \right)^2 \right]$
	Second mode	$V_{2,\max}(z) = 0.1265[S_a(T_1/3)] \left(\frac{W_{\text{trib}}}{g} \right) \left \cos 4.49 \left(\frac{z}{H} \right) + 0.217 \right $
	Third mode	$V_{3,\max}(z) = 0.0297[S_a(T_1/5)] \left(\frac{W_{\text{trib}}}{g} \right) \left \cos 7.73 \left(\frac{z}{H} \right) - 0.1283 \right $
Overturning moment	First mode	$M_{1,\max}(z) = M_{b,\max} \left[1 - \frac{3}{2} \left(\frac{z}{H} \right) + \frac{1}{2} \left(\frac{z}{H} \right)^2 \right]$
	Second mode	$M_{2,\max}(z) = 0.0282[S_a(T_1/3)] \left(\frac{W_{\text{trib}}}{g} \right) H \left \sin 4.49 \left(\frac{z}{H} \right) + 0.976 \left(\frac{z}{H} \right) \right $
	Third mode	$M_{3,\max}(z) = 0.00384[S_a(T_1/5)] \left(\frac{W_{\text{trib}}}{g} \right) H \left \sin 7.73 \left(\frac{z}{H} \right) - 0.991 \left(\frac{z}{H} \right) \right $

Using the first three modes, the modal contributions are combined by assuming that the peak response is reached in the first mode and sustained, and that the higher modes are superimposed on that first-mode response but are statistically independent of one another

$$V_{\max}(z) = V_{1,\max}(z) + \sqrt{[V_{2,\max}(z)]^2 + [V_{3,\max}(z)]^2} \quad (3)$$

$$M_{\max}(z) = M_{1,\max}(z) + \sqrt{[M_{2,\max}(z)]^2 + [M_{3,\max}(z)]^2} \quad (4)$$

Further discussion of these modal combinations is provided by Wiebe (2013).

Optional Method to Design Higher Mode Mitigation

The members of the CRSBF can be designed for the forces associated with the design envelopes given in Eqs. (3) and (4), as described later. However, if the higher modes dominate the design envelopes (i.e., the second term of Eq. (3) or (4) is greater than the first term), the designer may wish to consider mitigating the higher mode effects. Wiebe et al. (2013a, b) experimentally validated two techniques for doing this: designing multiple rocking joints and designing a nonlinear brace at the first story. This paper considers the design of either an upper rocking joint or nonlinear braces at the first story, but a similar approach can be used to design multiple additional rocking joints or nonlinear braces.

Design of Upper Rocking Joint

To be effective, an upper rocking joint must activate at a load that is both low enough to limit the response in the higher modes and also high enough to prevent the deformation demand for the system from concentrating at the upper rocking joint. To meet the latter requirement, the following two conditions are proposed:

$$M_{\text{upper,rock}} \geq M_{b,\text{rock,max}} \times \left[1 - \frac{3}{2} \left(\frac{z_{\text{upper}}}{H} \right) + \frac{1}{2} \left(\frac{z_{\text{upper}}}{H} \right)^2 \right] \quad (5)$$

$$\beta_{\text{upper}} \geq \beta_b \quad (6)$$

where $M_{\text{upper,rock}}$ = rocking moment at the upper rocking joint; $M_{b,\text{rock,max}}$ = maximum expected base rocking moment [Eq. (2), but replacing ED_θ and PT_θ with the forces in the energy dissipation and posttensioning elements, respectively, at $\theta = 0$ instead of $\theta = \theta_{\max}$]; z_{upper} = height of the upper rocking joint above the base rocking joint, and β_{upper} and β_b = energy dissipation parameters at

the upper and base rocking joints, respectively. The right side of Eq. (5) is the overturning moment at the upper rocking joint when the base moment is equal to the maximum expected base rocking moment, assuming an inverted triangular distribution of lateral forces. Once the target values for $M_{\text{upper,rock}}$ and β_{upper} have been determined, the upper rocking joint can be designed in the same way as the base rocking joint (Wiebe and Christopoulos 2014), using only the weight above the upper joint to calculate W_{self} and W_{trib} . To maximize the effectiveness of the upper joint, it is recommended that Eqs. (5) and (6) be satisfied with as little margin as is practicable.

Modification of Design Envelopes to Account for Influence of Upper Rocking Joint

After the upper rocking joint has been designed, the force demands on the other members of the CRSBF must be determined, accounting for the beneficial effect of the upper joint. As shown schematically in Fig. 2, it is proposed to estimate first-mode contribution to the overturning moment envelope as bilinear between the resistance of the base rocking joint at θ_{\max} , the resistance of the upper rocking joint at the maximum expected upper joint rotation, and zero at the roof. The maximum expected base rotation is assumed to be unaffected by the presence of the upper joint, and the maximum expected upper joint rotation is assumed to be equal to the maximum expected base rotation. Next, the contributions from the higher modes are estimated using the equations from Table 1 as though the two sections of the controlled rocking system were separate [i.e., calculating (z/H) as a fraction of the height of the section being considered and using only W_{trib} for that section]. The modal moment contributions are then combined using Eq. (4).

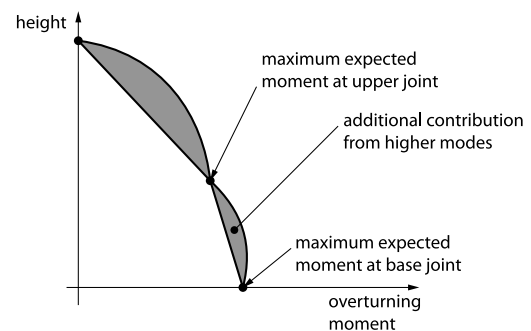


Fig. 2. Schematic moment design envelope for controlled rocking steel braced frame with two rocking joints

The same assumptions were found to result in poor estimates of the shear force envelope. Instead, it is proposed to estimate the contribution from the first mode as being equal to what it was estimated as for the system with rocking only at the base, while estimating the contributions from the higher modes as half of what they were with rocking only at the base (i.e., dividing the expressions that are given in Table 1 for the higher-mode contributions by two). The modal shear contributions are then combined using Eq. (3).

Once the overturning moment and shear envelopes have been determined, the member design demands are calculated in the same way as is recommended when rocking occurs only at the base. The upper rocking joint is detailed in a similar way as the base rocking joint.

Design of Nonlinear Brace(s)

Another higher mode mitigation technique is to replace the braces in one story with braces that are intended to behave nonlinearly. Since the brace force demands are related to the story shears, which are largest at the base, this paper only considers nonlinear braces in the first story. To avoid undesirable residual deformations and damage to the system, only self-centering energy dissipative (SCED) braces (Christopoulos et al. 2008) are considered.

Like an upper rocking joint, a nonlinear brace must activate at a load that is both low enough to limit the response in the higher modes and also high enough to prevent the deformation demand for the system from concentrating in the brace. To meet the latter requirement, the following condition is proposed:

$$F_{\text{act}} \geq F_{\text{brace}} |_{V_{b,\text{brace design}}} \quad (7)$$

where F_{act} = activation force for the nonlinear brace; and where $F_{\text{brace}} |_{V_{b,\text{brace design}}}$ = force in that brace at the design base shear for brace design, given in Eq. (8). Preliminary analyses showed that the deformation demand at the first-story level may be excessive if the SCED is designed to activate at the same base shear that causes rocking under an inverted triangular distribution of loads. Therefore, it is proposed that 25% of the second-mode design base shear from Table 1 be added to obtain the design base shear associated with the activation load

$$V_{b,\text{brace design}} = 1.5 \times (M_{b,\text{rock}}/H) + 0.25 \times V_{2,\text{max}}(z=0) \quad (8)$$

As shown later, this assumption led to desirable results for the analyses considered in this paper. The factor of 1.5 in Eq. (8) is derived from the assumed inverted triangular force distribution in the first mode and is not related to the design acceleration spectrum.

The energy dissipation parameter is proposed to be at least

$$\beta_{\text{SCED}} \geq 0.8 \quad (9)$$

Although it may not be necessary for the nonlinear brace to have any energy dissipation capacity, this has not been considered within the scope of this work. The proposed value for β_{SCED} is slightly less than the value used by Tremblay et al. (2008b), but it is consistent with the lower-bound values used by Erochko (2013). To prevent damage to the nonlinear brace, it is proposed to connect it using an external fuse that slips at the brace deformation that corresponds to a first-story drift of 1%. External fuses, consisting of slip-critical slotted connections, have been proposed by Tremblay et al. (2008b) and validated by Erochko et al. (2013).

Modification of Design Envelopes to Account for Influence of Nonlinear Brace(s)

Once the nonlinear brace has been designed, the force demands on the other members of the CRSBF must be determined, accounting for the beneficial effect of the nonlinear brace. To calculate the shear force and overturning moment design envelopes, it is proposed to estimate the contribution from the first mode as being equal to what it was calculated as for the system with linear brace elements (Table 1). Since the force in the nonlinear brace is limited by the external fuse, the maximum base shear is limited directly to $V_{b,\text{slip}}$. Therefore, it is proposed to scale the second-mode envelopes such that the total base shear from the first two modes is equal to the maximum base shear permitted by the nonlinear brace. That is, the second-mode envelopes from Table 1 are multiplied by the higher mode reduction factor ν

$$\nu = \frac{V_{b,\text{slip}} - 1.5 \times M_{b,\text{max}}/H}{V_{2,\text{max}}(z=0)} \geq 0 \quad (10)$$

where $M_{b,\text{max}}$ and $V_{2,\text{max}}(z=0)$ are given by Eq. (2) and in Table 1, respectively. The nonlinear brace is unlikely to be effective unless $V_{b,\text{slip}}$ is small enough that ν is less than one. Because the second mode is assumed to cause the nonlinear brace to reach its maximum possible load, the third and higher modes are assumed not to generate any additional force demand. The modal contributions are combined using Eqs. (3) and (4).

Design of Frame Elements, Shear Transfer Devices, Diaphragms, and Collectors

After the design shear and overturning moment envelopes have been calculated as described above, they are used to calculate the elastic force demands on the frame elements and shear transfer devices. There is no single lateral force distribution that is associated with all capacity design forces, just as there is no single lateral force distribution that is associated with all response quantities in a conventional response spectrum analysis. To calculate the capacity design demands for each brace element from the design shear force envelope, the larger of the shear force demands at the top and bottom of each story is used. Similarly, to determine the capacity design demands for each vertical element, the larger of the overturning moment demands at the top and bottom of each story is used. In addition, local effects from posttensioning and energy dissipation anchorages, as well as from rocking, must be considered.

Sliding may occur in response to shear at a rocking joint, and because it is not associated with a restoring force, it results in residual deformations that should be prevented at the immediate occupancy (IO) performance level. At the collapse prevention (CP) performance level, although sliding may be desirable (Sideris et al. 2014), this has not yet been studied for CRSBFs and therefore is not proposed to be permitted at any considered level of seismic response or wind loading. Likewise, although some studies of controlled rocking concrete walls have suggested that sliding can be prevented simply by verifying adequate frictional resistance (e.g., Kurama et al. 1999), this is not recommended because it has not been validated in dynamic tests of any CRSBF. The rocking joint should be designed to transfer the maximum shear that is expected at the CP performance level, computed using Eq. (3), while the joint rotation is equal to the maximum rotation permitted by the lock-up device. A bumper system is recommended for transferring this shear because it has been validated in several studies (Roke et al. 2010; Ma et al. 2011; Wiebe 2013; Eatherton et al. 2014).

Floor diaphragms and collector elements must be designed for the expected peak floor accelerations at the CP performance level. The floor acceleration envelope can be calculated in a similar way to the shear and moment envelopes, as described by Wiebe (2013).

After the members of the frame have been designed, the deflections under wind loading can be checked in the same way as for a conventional nonuplifting frame because the frame is designed to avoid uplift under wind loads.

The members of a CRSBF are not intended to dissipate seismic energy by yielding or buckling. Therefore, although failure of the connections between the members of a CRSBF would likely lead to a major loss of lateral load resistance, it is considered adequate to design the frame connections for the same forces as the frame members. Similarly, the beams in a chevron-braced frame need not be designed for the unbalanced forces associated with buckling of the compression brace.

Design of Prototype Structures

Designs without Higher Mode Mitigation

The proposed capacity design method was applied to frames with two, six, and 12 stories. These frames were designed to rock at loads associated with force reduction factors of 9, 30, and 16.3 relative to an MCE-level design spectrum. The two-story and six-story frames were designed to achieve the maximum possible energy dissipation while remaining self-centering, and the 12-story frame was designed with no supplemental energy dissipation. Part I (Wiebe and Christopoulos 2014) gives further details regarding the building properties, the design spectrum, the ground-motion suites, and the base rocking joint designs.

The purpose of the proposed capacity design method is to provide an acceptable level of certainty that frame members will respond in the elastic range. Therefore, the capacity design demands were not based on the median acceleration spectrum from the ground-motion suite, but instead were based on the 84th-percentile acceleration spectrum, which was calculated assuming a lognormal distribution of spectral accelerations at each period. Fig. 3 summarizes the story shear and overturning moment capacity design envelopes that were used to design the members. The final designs for the frames without higher mode mitigation are shown in Fig. 6 of Part I (Wiebe and Christopoulos 2014).

Designs with Higher Mode Mitigation

The capacity design envelopes for the two-story frame [Fig. 3(a)] were dominated by the first mode, but the envelopes for the six-story and 12-story frames [Figs. 3(b and c)] were dominated by the second mode, which is not limited by the base rocking mechanism. Therefore, alternative designs were also considered to mitigate the higher mode effects in these frames.

For the six-story frame, a second rocking joint was designed at the second floor level, where the overturning moment was largest [Fig. 3(b)]. No change was made to the base rocking joint, the post-tensioning was continued over the full frame height, and the same energy dissipation device was specified at the upper joint as at the base to achieve the desired overturning moment resistance and energy dissipation.

For the 12-story frame, a second rocking joint was designed at the fifth floor level, where the overturning moment was largest [Fig. 3(c)]. Allowing a gap to open at this level while transferring the story shear was the only required change according to the recommendations of this paper; no supplemental energy dissipation was provided at the upper rocking joint.

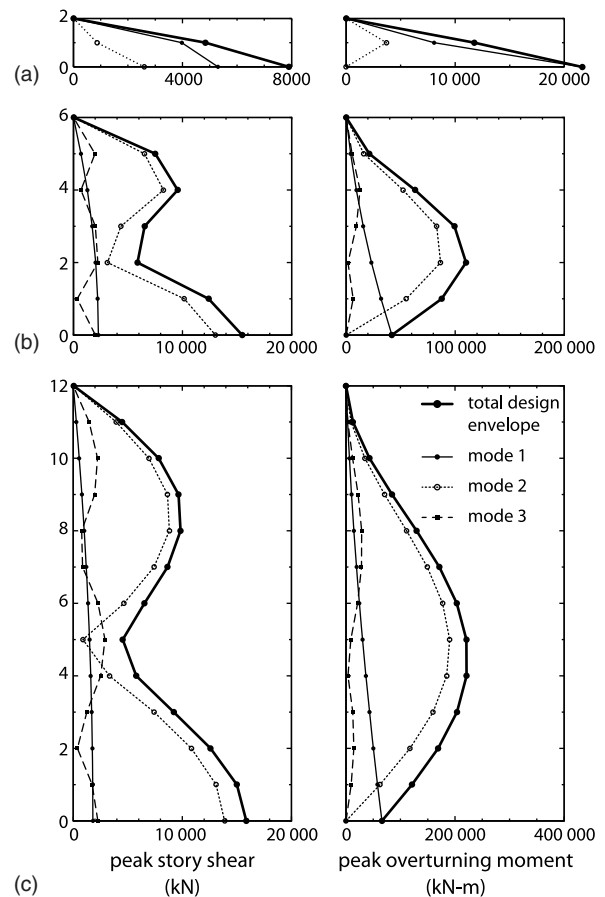


Fig. 3. Capacity design envelopes: (a) two-story frame; (b) six-story frame; (c) 12-story frame

The 12-story frame was also redesigned with self-centering energy dissipating (SCED) braces. A preliminary SCED brace design was evaluated using the SCED mechanics simulator developed by Erochko (2013) and found to have an activation load of 3,100 kN, an initial stiffness of 1,550 kN/mm, a postactivation stiffness ratio of $\alpha = 0.06$, and an energy dissipation parameter of $\beta = 1$. To prevent damage to the SCED brace due to excessive deformation demand, the brace was designed to be connected using a slip-critical slotted connection that serves as an external fuse. The fuse is specified to slip at a brace elongation of 30 mm, which corresponds to a first-story drift of 1.0% and a brace force of 5,700 kN.

Fig. 4 compares the capacity design envelopes for the six-story and 12-story frames with and without higher mode mitigation. When the frames were redesigned for the reduced forces, the total amount of steel was reduced by 26% for the six-story frame, and by 39 and 40% for the 12-story frames with two rocking sections and with a SCED brace, respectively.

The members of all frames were able to carry the factored wind loads, and the deflection of each frame at the serviceability level was less than 0.25% of the height of that frame.

Seismic Response of Prototype Structures

Modeling of Structure and Selection of Ground Motions

The six frames were modeled using *OpenSees* and subjected to suites of 44 records at the MCE and design basis earthquake

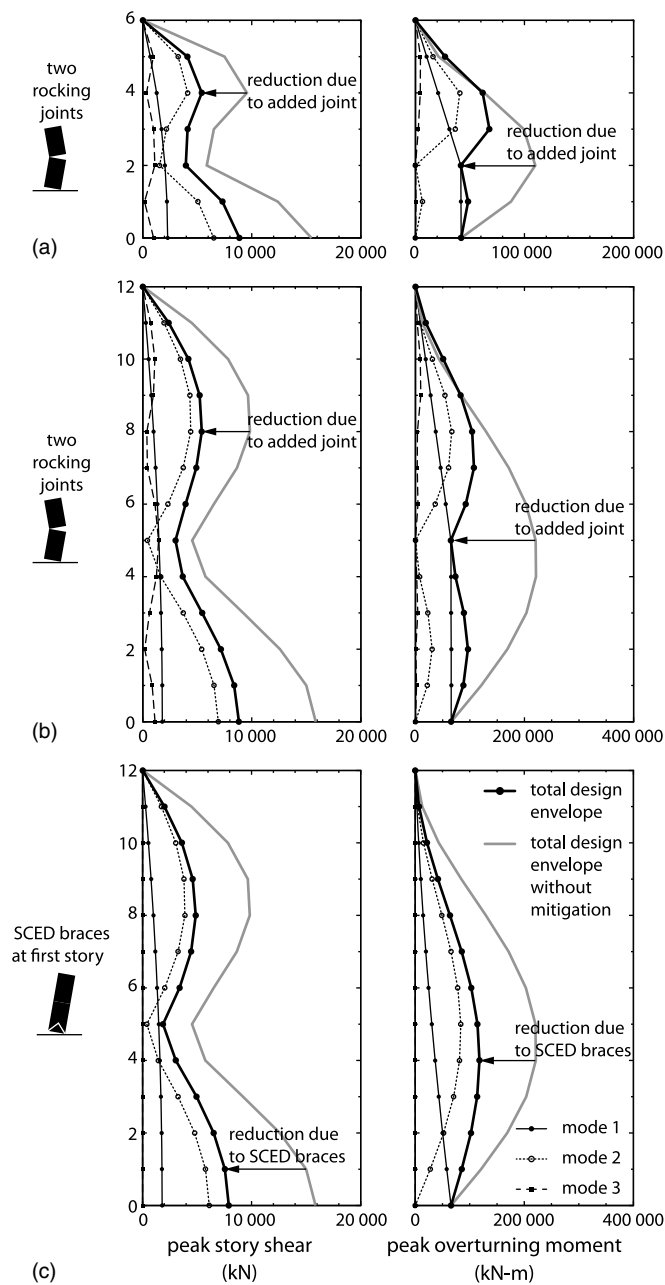


Fig. 4. Capacity design: (a) six-story frame with two rocking joints; (b) 12-story frame with two rocking joints; (c) 12-story frame with SCED brace at first story

(DBE) levels, in the same way as described in Part I (Wiebe and Christopoulos 2014). The SCED braces were modeled using corotational trusses with the self-centering material, where the properties were given in the previous section. The first-mode period of the six-story frame with two rocking joints was 1.14 s, and the first-mode periods of the 12-story frames with two rocking joints and with SCED braces at the first story were 2.24 s and 2.09 s, respectively. One out of 44 MCE-level records caused instability in the numerical models of both 12-story frames with higher mode mitigation after they reached a roof displacement of approximately 10%. This record is not included in the following results; however, such collapses may be preventable by including a lock-up device, as recommended in Part I (Wiebe and Christopoulos 2014). The influence of any

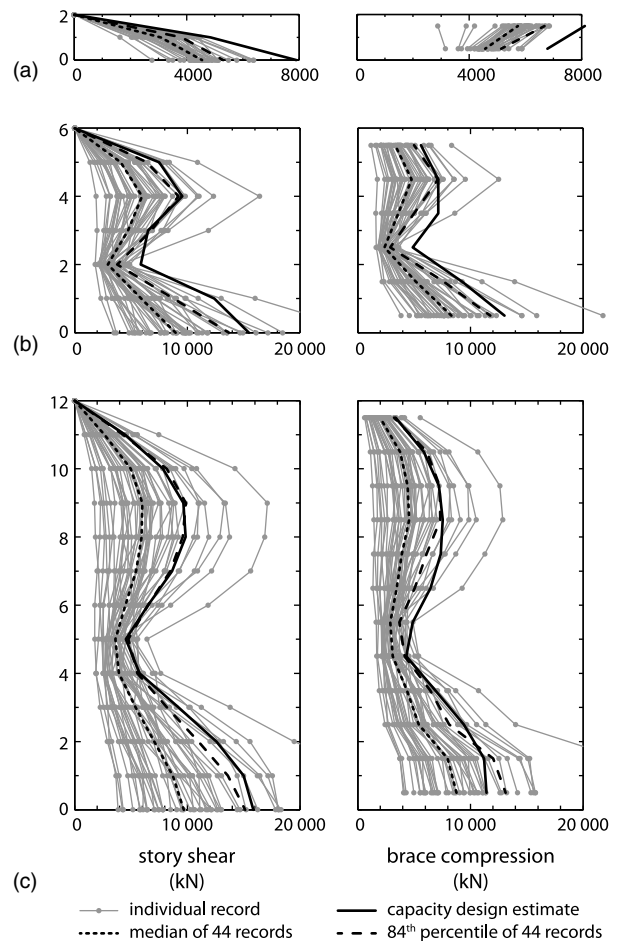


Fig. 5. Peak story shears and brace compressions during MCE suite of records: (a) two-story frame; (b) six-story frame; (c) 12-story frame. Each point on the story shear envelope represents the constant shear in the story above

unintended member nonlinearity was not considered in this study.

Story Shears and Brace Forces

The left side of Fig. 5 shows the peak story shears for the frames without higher mode mitigation during the MCE suite of records. The shears at each time step were calculated as the sum of the contributions from the braces and the column shears. The peak story shears of the two-story frame were overestimated by the proposed capacity design method, although they would be captured well if the method had not included the second mode. This is because the design equations in Table 1 are based on a cantilevered shear beam with uniformly distributed mass and stiffness (Wiebe 2013), and this approximation is unnecessarily conservative for such a low-rise building. However, the design envelope captures the 84th-percentile story shear envelopes reasonably well for the taller frames. A less conservative spectrum could be used to generate less conservative capacity design forces, but some degree of conservatism is appropriate because the design intent is to avoid damage to the structural elements.

During design, the peak story shears were assumed to be carried entirely by the braces, and the analytical results confirmed that the braces carried more than 95% of the story shear in almost all cases. The right side of Fig. 5 compares the peak brace forces from the

nonlinear time-history analyses to the design estimates. Like the estimates of the peak story shears, the capacity design estimates of the peak brace forces are quite conservative for the two-story frame, but similar to the 84th-percentile results for the six-story and 12-story frames. The capacity design estimates correctly capture that the force is larger at the upper level of the two-story frame than at the lower level. The estimates also correctly capture the reduction in peak brace forces that occurs below midheight of the six-story and 12-story frames because of the properties of the second mode, despite not requiring a modal analysis of the frame.

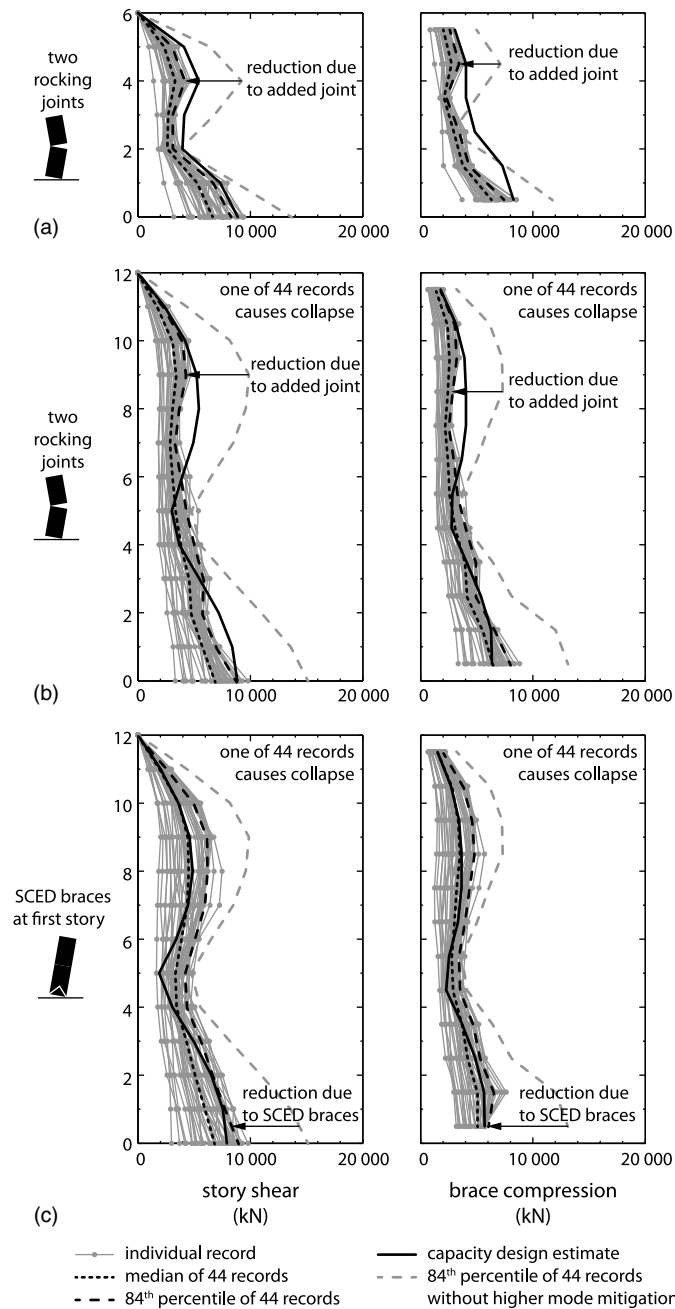


Fig. 6. Peak story shears and brace compressions during MCE suite of records: (a) six-story frame with two rocking joints; (b) 12-story frame with two rocking joints; (c) 12-story frame with SCED braces at first story. Each point on the story shear envelope represents the constant shear in the story above

The left side of Fig. 6 shows the peak story shears during the MCE suite of records for the frames with multiple mechanisms. For the six-story frame, the 84th-percentile peak base shear was reduced by 40% by adding an upper rocking joint, and the shears were reduced elsewhere in the frame as well. The design method was conservative, predicting peak shears that exceeded the 84th-percentile response from the numerical analyses. For the 12-story frame with two rocking sections, the 84th-percentile base shear was reduced by 42% relative to the system with rocking at the base only; a 41% reduction was achieved by using a SCED brace at the first story. The design method was less conservative than intended at the fourth and fifth stories for the 12-story frame with two rocking joints and at most levels of the 12-story frame with SCED braces. For all three systems, adding higher mode mitigation greatly reduced the record-to-record variability of the shear force envelopes relative to the systems that relied on base rocking alone to limit the forces.

The right side of Fig. 6 shows a commensurate reduction in peak brace compressive forces when higher mode mitigation is used. The proposed design method for frames with two rocking sections produces conservative estimates of the 84th-percentile peak brace compression forces at most levels. For frames with a SCED brace at the first story, the proposed design method is less conservative but still produces reasonable estimates of the peak brace forces at most levels.

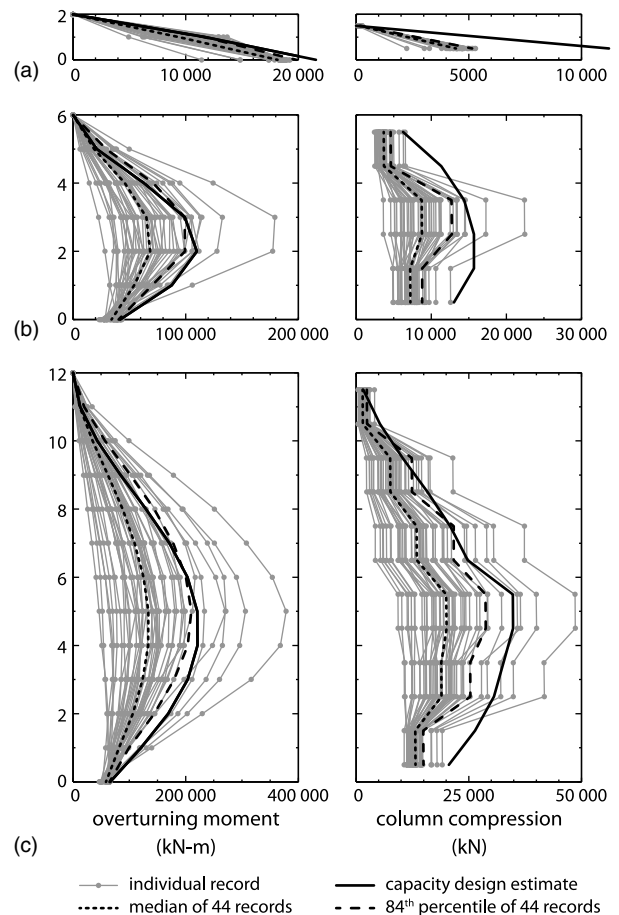


Fig. 7. Peak overturning moments and column compressions during MCE suite of records: (a) two-story frame; (b) six-story frame; (c) 12-story frame

Overturning Moments and Column Forces

The left side of Fig. 7 shows the peak overturning moments during the MCE suite of records for the frames with rocking at the base only, calculated from the member forces. The base overturning moment is not influenced by the higher modes, and it was slightly overestimated for all three frames by assuming the maximum possible forces in the posttensioning and energy-dissipation elements. For the two-story frame, the capacity design envelope is only slightly larger than the 84th-percentile envelope. The second mode could have been neglected without a pronounced influence on the capacity design forces. For the taller frames, the design

envelope tends to slightly overestimate the 84th-percentile moments in the lower half of the frame and to slightly underestimate them in the upper half. However, the agreement is considered to be good, considering the simplicity of the design approach.

During design, the frame overturning moments were assumed to be carried by a column axial force couple. The columns also carry compression due to the posttensioning force and the self-weight of the frame. The right side of Fig. 7 shows that the capacity design estimates are conservative relative to the 84th-percentile results for all three frame heights. These design forces are more conservative than the peak moments because of the conservative design assumption that the posttensioning reaches its ultimate strength and because the design forces are based on the maximum overturning

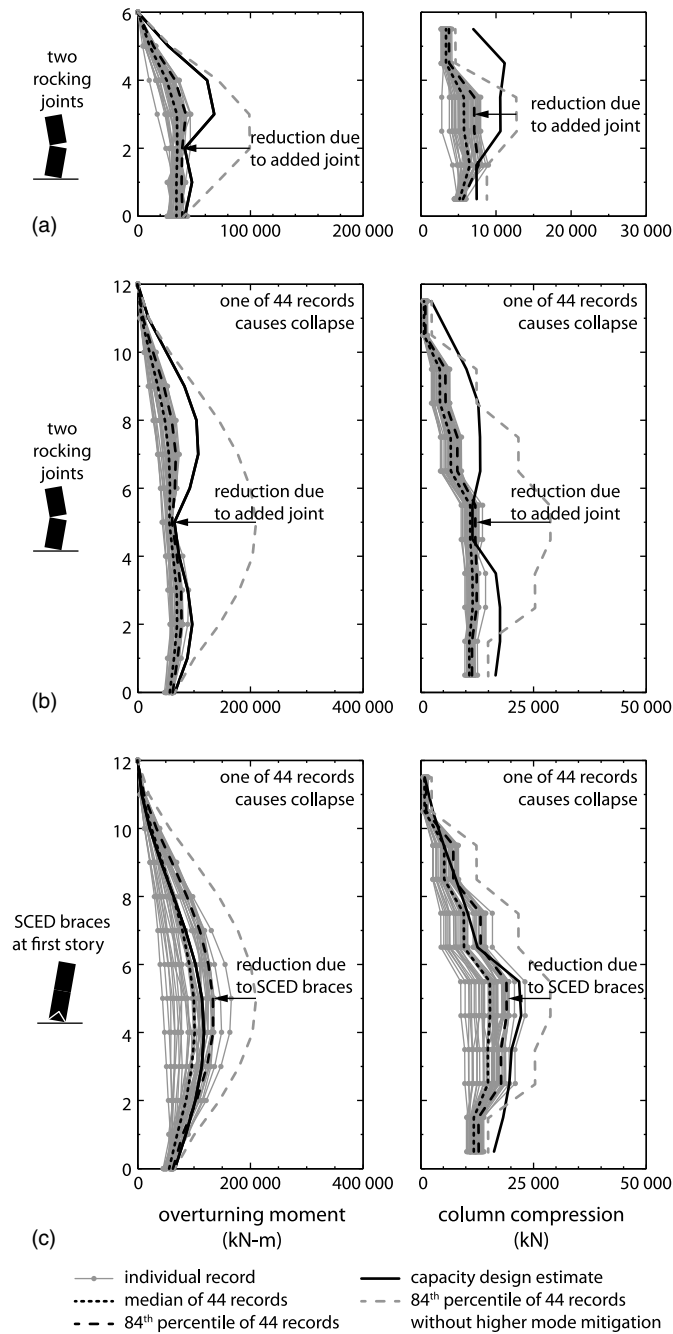


Fig. 8. Peak overturning moments and column compressions during MCE suite of records: (a) six-story frame with two rocking joints; (b) 12-story frame with two rocking joints; (c) 12-story frame with SCED braces at first story

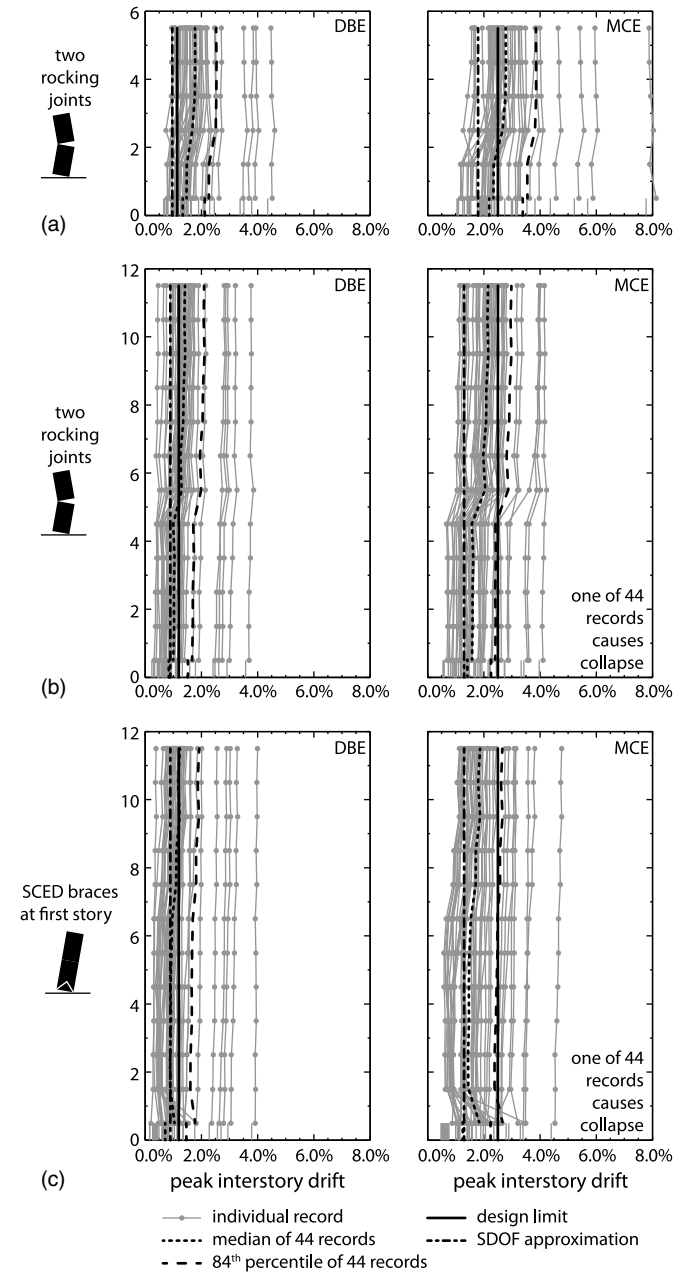


Fig. 9. Peak interstory drifts and base rotations during DBE and MCE records: (a) six-story frame with two rocking joints; (b) 12-story frame with two rocking joints; (c) 12-story frame with SCED braces at first story

moment over each story, even though the axial force in each column can change only where braces are connected (i.e., every second story). Despite this conservatism, some records cause peak column compression demands that are well in excess of the estimated demands for the six-story and 12-story frames.

The left side of Fig. 8 shows the peak overturning moments during the MCE suite of records for the frames with higher mode mitigation. Although the peak base overturning moments were similar for frames with and without multiple mechanisms, the moments above the base were reduced by using multiple mechanisms: adding an upper joint reduced the maximum 84th-percentile moments over the heights of the six-story and 12-story frames by 57% and 62%, respectively, while replacing the first-story braces with SCED braces reduced the maximum 84th-percentile moment over the height of the 12-story frame by 36%. When two rocking joints were used, the capacity design envelopes were very conservative relative to the 84th-percentile response. When SCED braces were used at the first story, the capacity design envelope was generally less than one standard deviation on the conservative side of the median response, which was slightly less conservative than intended.

The peak column compressions for the frames with multiple mechanisms are shown on the right side of Fig. 8. Using multiple mechanisms reduced the maximum 84th-percentile column compression demands over the height by as much as 56%. The capacity design estimates of the peak column forces exceeded the 84th-percentile response with two rocking sections and were generally greater than or close to the 84th-percentile response for the 12-story frame with a SCED brace. The record-to-record variability for peak column compressive forces was substantially reduced by implementing higher mode mitigation.

Peak Interstory Drifts

Fig. 9 shows the peak interstory drifts for the frames with higher mode mitigation during the DBE-level and MCE-level records. In general, the peak interstory drifts are larger for the frames with higher mode mitigation than they were for the frames without mitigation [Fig. 8 in Wiebe and Christopoulos (2014)] because the frames with higher mode mitigation used less steel, resulting in longer periods. For the six-story frame, adding an upper rocking joint increased the maximum of the median peak interstory drifts by 32% at the DBE level and 35% at the MCE level. As a result, the median peak interstory drifts at some levels exceeded the design limits that

were set in Part I (Wiebe and Christopoulos 2014) for both suites of ground motions. These results were not captured very well by the single-degree-of-freedom (SDOF) model that was discussed in Part I (Wiebe and Christopoulos 2014) because that model did not allow for any rotation at the upper rocking joint. In addition, the SDOF model assumed that the supplemental energy dissipation had an elastic-perfectly-plastic response, whereas these analyses included the Bauschinger effect.

For the 12-story frame, adding an upper rocking joint increased the maximum of the median peak interstory drifts by 24% at the DBE level and 27% at the MCE level, while replacing the first-story braces with SCED braces increased the maximum of the median peak interstory drifts by 8% at the DBE level and 10% at the MCE level. The median peak interstory drifts for the 12-story frame without higher mode mitigation were much less than the design limits that were set in Part I (Wiebe and Christopoulos 2014), so the median interstory drifts only exceeded the design limits at the DBE level for the frame with two rocking joints. The median peak base rotations of the 12-story frames with higher mode mitigation were captured reasonably well by the SDOF models that were discussed in Part I (Wiebe and Christopoulos 2014), using the first-mode periods from the numerical models. Although the SDOF model captures the median DBE-level interstory drifts reasonably well, the maximum of the median peak interstory drifts at the MCE level are about 50% more than the SDOF approximation for both of the 12-story frames with multiple mechanisms. This is because the MCE-level records cause more deformation in the higher mode mitigation mechanisms.

SCED Brace Elongation and Global Uplift

Table 2 shows that the SCED braces, which were each designed with an external fuse that activates and reduces the brace stiffness to zero after the brace reaches an elongation of 30 mm, had a median peak elongation of 11.7 mm at the DBE level. At the MCE level, the median brace elongation was 25.0 mm, but the external fuse was activated frequently enough that the 84th-percentile elongation was 55.2 mm. This amount of slip could easily be accommodated by a slotted connection, so it is considered to be consistent with the design intent. The SCED braces were generally effective in limiting the system forces without attracting excessive deformation demand, confirming that the coefficient of 0.25 in Eq. (8) was appropriate for this design.

Table 2. Peak Global Uplift, Upper Joint Rotations, Posttensioning Strains, and SCED Brace Elongations

Design	Parameter	DBE		MCE	
		DBE median	84th percentile	MCE median	84th percentile
Six stories, rocking only at base	Global uplift	0.0 mm	0.1 mm	0.0 mm	1.0 mm
	Posttensioning strain	0.61%	0.83%	0.80%	1.16%
Six stories, two rocking joints	Base joint global uplift	0.0 mm	0.1 mm	0.6 mm	26.5 mm
	Upper joint rotation	0.94%	1.84%	1.67%	3.15%
	Upper joint global uplift	0.0 mm	0.0 mm	0.2 mm	5.7 mm
	Posttensioning strain	0.76%	0.98%	1.08%	1.43%
12 stories, rocking only at base	Global uplift	0.0 mm	0.0 mm	0.0 mm	0.0 mm
	Posttensioning strain	0.73%	0.93%	0.89%	1.20%
12 stories, two rocking joints ^a	Base joint global uplift	0.0 mm	0.0 mm	0.0 mm	0.0 mm
	Upper joint rotation	0.38%	2.38%	0.95%	2.42%
	Upper joint global uplift	0.0 mm	0.0 mm	0.0 mm	0.0 mm
	Posttensioning strain	0.82%	1.01%	1.03%	1.27%
12 stories, SCED braces at first story ^a	Global uplift	0.0 mm	0.0 mm	0.0 mm	0.0 mm
	SCED elongation	11.7 mm	25.6 mm	25.0 mm	55.2 mm
	Posttensioning strain	0.73%	0.95%	0.89%	1.16%

^aOne of 44 records caused collapse and is excluded from these calculations.

When two rocking joints were used, the 84th-percentile global uplift at the base rocking joint of the six-story frame was 26.5 mm at the MCE level (Table 2), which was much larger than for the design with rocking only at the base and which may be significant for the design of the energy dissipation device. Nevertheless, the median peak global uplift was less than 1 mm at both rocking joints, which suggests that relaxing Eq. (15) in Wiebe and Christopoulos (2014) did not generally have a detrimental effect on the performance of the system.

Residual Displacements

Fig. 10 shows the residual displacements of the frames with higher mode mitigation. The mean residual displacements of the six-story frame were increased by adding an upper rocking joint [see Fig. 8(b)]

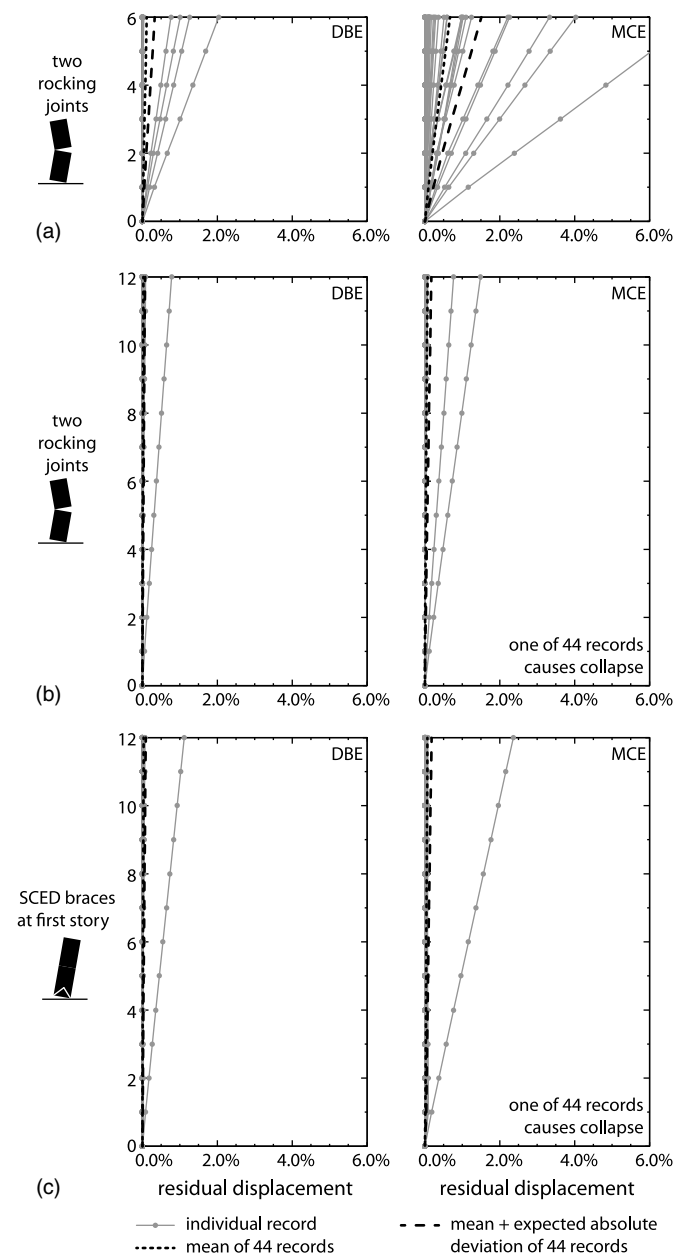


Fig. 10. Residual displacements after DBE and MCE records: (a) six-story frame with two rocking joints; (b) 12-story frame with two rocking joints; (c) 12-story frame with SCED braces at first story

in Wiebe and Christopoulos (2014)] because the upper rocking joint was sometimes sufficiently active to yield the posttensioning, reducing the recentering capability. For the 12-story frames with multiple mechanisms, the residual displacements were less than 0.2% for almost all records, but the records that caused residual drifts for the frames with rocking at the base only [Fig. 8(c) in Wiebe and Christopoulos (2014)] caused larger residuals or collapse.

Conclusion

The peak forces in the members of a controlled rocking steel braced frame may be dominated by the higher modes of seismic response. Higher mode effects are likely to be particularly significant for tall frames, especially if the system is designed with a large force-reduction factor, as recommended in Part I (Wiebe and Christopoulos 2014). This paper presented a method to estimate the elastic force demands on the elements of a CRSBF, including the influence of higher mode effects. This method can be implemented in a spreadsheet easily, and it can be used for preliminary design purposes because it requires only building properties that are known before a trial design has been developed.

This paper validated the proposed capacity design method by applying it to example designs with two, six, and 12 stories. The capacity design method generally captured the 84th-percentile story shears and overturning moments. The method was based on the 84th-percentile spectrum of ground motions, but a different percentile of force demands could be targeted by adjusting the spectrum used. The method was more conservative than intended for the shears in the two-story frame and for translating the overturning moment envelope into column compression forces. Ongoing research seeks to address these issues.

For situations where higher mode effects dominate the design forces, this paper also proposed a new design method for mitigating these effects by using multiple mechanisms. The nonlinear time-history analyses presented here verified that the peak frame forces can be greatly reduced by using higher mode mitigation. Considering the simplicity of the approach, the proposed method gives a reasonable estimate of the force reduction, although the method was generally more conservative than intended for the frames with two rocking joints and less conservative than intended for the frame with nonlinear braces at the first story. The peak interstory drifts of the frames with multiple mechanisms were generally somewhat more than for the frames with rocking at the base only, but the drifts still satisfied the design limits in most cases. The residual displacements were negligible after most records. However, one record caused the 12-story frame with higher mode mitigation to collapse. This may have been prevented by including a lock-off device to prevent excessive base rotations. Using multiple mechanisms allowed the six-story frame to be designed with 26% less steel than the design with rocking at the base only, while about 40% less steel was needed for the 12-story frames.

All of the designs considered in this paper were based on separating the CRSBF from the gravity load carrying system, such that each CRSBF carried only its own weight. Although this avoids possible amplification of column forces after impact, the connections between the floor and frame systems are critical and should be validated experimentally. The models also assumed that all elements, except the posttensioning and supplemental energy dissipation, responded in the linear elastic range, even though the design forces for the elements were exceeded during approximately 15% of the ground motions. The influence of any inelastic frame behavior was not investigated in this study. Ongoing research seeks

to further validate the proposed design methodology by applying it to more buildings, investigating the influence of gravity loads carried by the CRSBF, and modeling the potential nonlinear behavior of frame elements during large events. Further study is also needed to evaluate the initial and life-cycle costs and benefits of implementing CRSBFs.

Acknowledgments

This project was funded by the Natural Sciences and Engineering Research Council of Canada, the Canadian Seismic Research Network, and the Ontario Ministry of Research and Innovation.

References

- ASCE. (2010). "Minimum design loads for buildings and other structures." *ASCE/SEI 7-10*, Reston, VA.
- Christopoulos, C., Tremblay, R., Kim, H.-J., and Lacerte, M. (2008). "Self-centering energy dissipative bracing system for the seismic resistance of structures: development and validation." *J. Struct. Eng.*, 10.1061/(ASCE)0733-9445(2008)134:1(96), 96–107.
- Eatherton, M., and Hajjar, J. (2010). "Large-scale cyclic and hybrid simulation testing and development of a controlled-rocking steel building system with replaceable fuses." *NSEL Rep. NSEL-025*, Univ. of Illinois at Urbana, Champaign, IL.
- Eatherton, M., Ma, X., Krawinkler, H., Deierlein, G., and Hajjar, J. (2014). "Quasi-static cyclic behavior of controlled rocking steel frames." *J. Struct. Eng.*, 10.1061/(ASCE)ST.1943-541X.0001005, 04014083.
- Erochko, J. (2013). "Improvements to the design and use of post-tensioned self-centering energy-dissipative (SCED) braces." Ph.D. thesis, Univ. of Toronto, Toronto.
- Erochko, J., Christopoulos, C., Tremblay, R., and Kim, H.-J. (2013). "Shake table testing and numerical simulation of a self-centering energy dissipative braced frame." *Earthquake Eng. Struct. Dyn.*, 42(11), 1617–1635.
- FEMA. (2009). "Quantification of building seismic performance factors." *Rep. FEMA P695*, Washington, DC.
- Gledhill, S. M., Sidwell, G. K., and Bell, D. K. (2008). "The damage avoidance design of tall steel frame buildings—Fairlie terrace student accommodation project, Victoria University of Wellington." *Proc., 2008 New Zealand Society Earthquake Engineering Conf.*, New Zealand Society for Earthquake, Wellington, New Zealand.
- Kurama, Y., Pessiki, S., Sause, R., and Lu, L.-W. (1999). "Seismic behavior and design of unbonded post-tensioned precast concrete walls." *PCI J.*, 44(3), 72–89.
- Kwon, O.-S., and Kim, E. S. (2010). "Evaluation of building period formulas for seismic design." *Earthquake Eng. Struct. Dyn.*, 39(14), 1569–1583.
- Latham, D. A., Reay, A. M., and Pampanin, S. (2013). "Kilmore street medical centre: Application of a post-tensioned steel rocking system." *Proc., Steel Innovations Conf. 2013*, Steel Construction New Zealand, Manuakau City, New Zealand.
- Ma, X., et al. (2010). "Seismic design and behavior of steel frames with controlled rocking—Part II: Large scale shake table testing and system collapse analysis." *Proc., ASCE/SEI Structures Congress 2010*, ASCE, Reston, VA.
- Ma, X., Krawinkler, H., and Deierlein, G. G. (2011). "Seismic design, simulation and shake table testing of self-centering braced frame with controlled rocking and energy dissipating fuses." *Rep. No. 174*, John A. Blume Earthquake Engineering Center, Stanford Univ., Stanford, CA.
- Mar, D. (2010). "Design examples using mode shaping spines for frame and wall buildings." *Proc., 9th U.S. and 10th Canadian Conf. Earthquake Engineering*, Earthquake Engineering Research Institute (EERI), Oakland, CA.
- Midorikawa, M., Azuhata, T., Ishihara, T., and Wada, A. (2006). "Shaking table tests on seismic response of steel braced frames with column uplift." *Earthquake Eng. Struct. Dyn.*, 35(14), 1767–1785.
- OpenSees v2.3.2 [Computer software]. Berkeley, CA, Pacific Earthquake Engineering Research Center.
- Pollino, M., and Bruneau, M. (2008). "Dynamic seismic response of controlled rocking bridge steel-truss piers." *Eng. Struct.*, 30(6), 1667–1676.
- Roke, D., Sause, R., Ricles, J. M., and Chancellor, N. B. (2010). "Damage-free seismic resistant self-centering concentrically-braced frames." *ATLSS Rep. 10-09*, Lehigh Univ., Bethlehem, PA.
- Roke, D., Sause, R., Ricles, J. M., and Gonner, N. (2009). "Damage-free seismic resistant self-centering steel concentrically-braced frames." *Proc., STESSA 2009*, CRC Press, London, 3–10.
- Sause, R., Ricles, J. M., Roke, D., Chancellor, N. B., and Gonner, N. P. (2010). "Seismic performance of a self-centering concentrically braced frames." *Proc., 9th US and 10th Canadian Conf. on Earthquake Engineering*, Toronto.
- Sideris, P., Aref, A. J., and Filiatrault, A. (2014). "Large-scale seismic testing of a hybrid sliding-rocking posttensioned segmental bridge system." *J. Struct. Eng.*, 04014025.
- Tait, J. D., Sidwell, G. K., and Finnegan, J. F. (2013). "Case study—Elevate apartments—A rocking 15 storey apartment building." *Proc., Steel Innovations Conf. 2013*, Steel Construction New Zealand, Manuakau City, New Zealand.
- Tremblay, R., et al. (2008a). "Innovative viscously damped rocking braced frames." *Proc., 14th World Conf. on Earthquake Engineering*, International Association for Earthquake Engineering (IAEE), Tokyo.
- Tremblay, R., Lacerte, M., and Christopoulos, C. (2008b). "Seismic response of multistory buildings with self-centering energy dissipative steel braces." *J. Struct. Eng.*, 10.1061/(ASCE)0733-9445(2008)134:1(108), 108–120.
- Wiebe, L., and Christopoulos, C. (2014). "Performance-based seismic design of controlled rocking steel braced frames. I: Methodological framework and design of base rocking joint." 10.1061/(ASCE)ST.1943-541X.0001202, 04014226.
- Wiebe, L., Christopoulos, C., Tremblay, R., and Leclerc, M. (2013a). "Mechanisms to limit higher mode effects in a controlled rocking steel frame. 1: Concept, modelling, and low-amplitude shake table testing." *Earthquake Eng. Struct. Dyn.*, 42(7), 1053–1068.
- Wiebe, L., Christopoulos, C., Tremblay, R., and Leclerc, M. (2013b). "Mechanisms to limit higher mode effects in a controlled rocking steel frame. 2: Large-amplitude shake table testing." *Earthquake Eng. Struct. Dyn.*, 42(7), 1069–1086.
- Wiebe, L. D. A. (2013). "Design of controlled rocking steel frames to limit higher mode effects." Ph.D. thesis, Univ. of Toronto, Toronto.